

Article

Assessing the Impact of Hg-Contaminated Sediments Washing through Sentinel Species: A Mesocosm Approach

Giuseppe Mancini ¹, Simone Cappello ², Giuseppe De Marco ^{3,*}, Tiziana Cappello ³, Maria Maisano ³, Rosalba Gornati ⁴, Massimiliano Scalici ⁵, Antonella Luciano ^{6,*}, Paolo Viotti ⁷ and Debora Fino ⁸

- ¹ Electric, Electronics and Computer Engineering Department, University of Catania, 5 Viale Andrea Doria 6, 95125 Catania, Italy; giuseppe.mancini@unict.it
 - ² Institute for Biological Resources and Marine Biotechnology (IRBIM)-National Research Center, Via S. Ranieri 86, 98122 Messina, Italy; simone.cappello@cnr.it
 - ³ Department of Chemical, Biological, Pharmaceutical and Environmental Sciences, University of Messina, Viale F. Stagno d'Alcontres 31, 98166 Messina, Italy; tcappello@unime.it (T.C.); mmaisano@unime.it (M.M.)
 - ⁴ Department of Biotechnology and Life Sciences, University of Insubria, Via Dunant 3, 21100 Varese, Italy; rosalba.gornati@uninsubria.it
 - ⁵ Department of Sciences, University of Roma Tre, Viale G. Marconi 446, 00146 Rome, Italy; massimiliano.scalici@uniroma3.it
 - ⁶ ENEA Italian National Agency for New Technologies Energy and Sustainable Economic Development, RC Casaccia, 00123 Rome, Italy
 - ⁷ Department of Civil, Building and Environmental Engineering, Sapienza University of Rome, Via Eudossiana 18, 00184 Rome, Italy; paolo.viotti@uniroma1.it
 - ⁸ Department of Applied Science and Technology (DISAT), Polytechnic of Turin, C.so Duca Degli Abruzzi 24, 10129 Turin, Italy; debora.fino@polito.it
- * Correspondence: gdemarco@unime.it (G.D.M.); antonella.luciano@enea.it (A.L.)

Abstract: This study combines a traditional chemical characterization with a simultaneous biological evaluation through histological, immunohistochemical, and enzymatic observations to assess the efficiency and sustainability of soil washing on Hg-contaminated sediment in terms of the bioavailability of the contaminant before and after the treatment, as well as the potential drawbacks of the treatment that are not revealed by a simple chemical characterization of treated sediments on its own. Different extracting agents, that is, ethylenedinitrilotetraacetic acid (EDTA), ethylenediaminedisuccinic acid (EDDS), sodium thiosulfate, potassium iodide (KI), and iodine (I₂), have been compared in this work to evaluate their efficiency in the removal of Hg from contaminated sediments. Speciation analysis was applied to assess the mobility of Hg from different fractions of aged sediments. Biological evaluation was carried out through the use of large mesocosms and *Mytilus galloprovincialis* as biological sentinels. Results from bench scale tests have shown Hg removal of up to 93% by means of the multi-step KI/I₂ washing process of the sediment. Results from histological, immunohistochemical, and enzymatic analysis have shown significant differences in the degree of alteration of biological tissues and their functional integrity between organisms in contact with contaminated and restored sediments. The reduction in 5-HT3R immunopositivity in the mesocosm with treated sediments suggests a tendency for mussels to recover a healthy condition. This result was also confirmed by the measurement of the enzymatic activity of AChE in mussel gills, which was significantly reduced in organisms from the mesocosm with polluted sediments compared with those from the one with restored sediments. The proposed approach could help stakeholders all over the world select, at an early stage, the most efficient cleaning action from a more holistic perspective, including not only pollutant concentration and economic reduction but also a direct assessment of the ultimate impact of the selected process on the biological system.

Keywords: sediments; mercury (Hg); soil washing; system biology; *Mytilus galloprovincialis*



Citation: Mancini, G.; Cappello, S.; De Marco, G.; Cappello, T.; Maisano, M.; Gornati, R.; Scalici, M.; Luciano, A.; Viotti, P.; Fino, D. Assessing the Impact of Hg-Contaminated Sediments Washing through Sentinel Species: A Mesocosm Approach. *Water* **2023**, *15*, 3258. <https://doi.org/10.3390/w15183258>

Academic Editor: Catherine N. Mulligan

Received: 28 July 2023

Revised: 30 August 2023

Accepted: 1 September 2023

Published: 13 September 2023



Copyright: © 2023 by the authors. Licensee MDPI, Basel, Switzerland. This article is an open access article distributed under the terms and conditions of the Creative Commons Attribution (CC BY) license (<https://creativecommons.org/licenses/by/4.0/>).

1. Introduction

Since the first industrial revolution, industries have provided means to improve our quality of life. Unfortunately, some of their emissions, side-products, and residues are inherently detrimental to the environment.

Because of its crucial geographical position, the Augusta Bay (Sicily, Italy) hosts one of the most important European industrial harbors. This quality led to the creation of one of the largest and most complex petrochemical districts in Europe in the early 1960s [1]. The Augusta Bay is currently considered a high environmental risk area due to its historical soil contamination and uncontrolled chemical discharges, which were legally allowed to take place before the implementation of the first Italian water pollution control law [2], and, on occasion, as a result of some industrial accidents [3]. As a result of the contamination of the air, seawater, and marine biota, the Italian Government has included the Augusta coastal area in the list of the Contaminated Sites of National Relevance (G.U.R.I., Law 426/1998).

The sediments of the Augusta Bay are highly contaminated by a variety of pollutants, including anthropogenic mercury, which has been discharged by a chlor-alkali plant since the 1960s [4–6]. An exhaustive study of the characteristics of mercury in sediments was provided by Salvagio et al. [7].

The sediments in the Augusta Bay, where some zones display Hg concentration values well above 100 mg/kg, have in turn induced significant contamination of the aquatic biota [8], which has been detected by means of organisms that are commonly used in biomonitoring metal pollution programs. In the past, this contamination was ascribed to the transformation of Hg into Methyl mercury, which is more toxic than inorganic mercury compounds and is the main cause of mercury biomagnification in fish [9,10]. Balance between the reduced and oxidized form of Hg essentially depends on redox reactions to these mediums.

It has also been shown that mercury-polluted sediments are a potential pollutant source for the Mediterranean ecosystem, as well as a potential risk for human health [1]. At the same time, they constitute a hindrance to the economic development of the area, as the depth of the bay is inadequate for the most recent tankers, and dredging is strongly limited in terms of authorizations.

These facts have pushed stakeholders to recognize the need for remediation action in the area [11,12]. However, an appropriate and holistic evaluation of the advantages and drawbacks of such an activity is still not available. Such an intervention could be complex, costly, and environmentally risky [13]. Therefore, it is essential to compare historic pollution and natural remediation actions, that have occurred over the last few decades, with any expected disturbance that could be induced on sediments via sea turbulence and human activities. Such a comparison would help to create a sustainable choice in view of expected industrial development limitations on harbor activities if limited or no interventions are introduced [14]. Moreover, a sustainable remediation approach needs to be defined in terms of economic and environmental burdens.

The usually adopted Hg-contaminated sediment management strategies [15] include natural attenuation, dredging followed by electrokinetics [16], phytoextraction [17], thermal desorption [18], soil washing [19–21], and stabilization/immobilization [11].

Treated sediments may then be returned to the same areas in the bay or used as fillers in a Confined Disposal Facility (CDF); alternatively, untreated sediments could be landfilled (a costly and partial solution).

Since each remedial action can result in a change in the physical, chemical, and biological conditions of the sediments [21], it is possible that the speciation and transport properties of mercury might change [22] as a result of a remedial action [23,24]. Each potential remediation operation should therefore be evaluated carefully, since each one can produce different benefits and risks, depending on the specific context in which it is applied.

The conventional concentration-limit approach, which is based on the chemical characterization of the impacted matrix, may not be sufficient to appropriately assess the post-remediation residual risks for ecosystems, as many local conditions (i.e., temperature, pH, redox potential, salinity, presence of organic substrate, etc.) can affect the bioavailability and toxicity of a pollutant. Furthermore, the distribution and availability of chemicals and by-products, as well as their potential interactions, may result in unexpected and unwanted effects on the ultimate toxicity of the treated sediment.

Integrating traditional analytic techniques with a simultaneous biological investigation could provide an early warning of the potential effects (positive or negative) of an adopted technological solution [25–27] before its implementation.

The use of sentinel organisms as biological models [28–31] allows for the bioavailability of pollutants and their potential risk of diffusion throughout the trophic network to be assessed [32] and for the response of the system to the remediation/depollution action to be predicted [33–36] at different biological organization levels [37,38].

Bivalve mollusks appear to be perfect biological models, as they are able to bioaccumulate and concentrate pollutants and are therefore able to provide evidence of both the chronic and fast effects [39] of bioremediation technologies on an impacted ecosystem [40–42].

This study had the aim of evaluating the possibility of sustainably removing Hg from Augusta Bay sediments. Specifically, the aim of this study was to (1) evaluate the distribution of mercury throughout different fractions of sediments (through a sequential extraction procedure); (2) evaluate the efficiency of a soil-washing treatment by comparing different leaching agents and establishing the required number of leaching cycles; (3) provide information on the environmental benefits/risks associated with the residual contamination of treated sediments through a mesocosm study using *M. galloprovincialis* as a bio-sentinel; and (4) propose a new approach—based on system biology—to help stakeholders in any part of the world identify the best strategy by selecting, at an early stage, the most efficient cleaning action from a more holistic and broad perspective, including not only a pollutant concentration and costs assessment, but also a direct assessment of the ultimate impact of the selected process on a biological system.

2. Materials and Methods

2.1. Sediments

The study area is represented in Figure 1a. Polluted sediments were sampled in the Augusta Bay (Syracuse, 37°10′39.20100″ N, 15°12′26.286″ E), while uncontaminated sediments were sampled in Brucoli (Syracuse, 37°17′23.67″ N, 15°12′40.68″ E), which was chosen as a reference site (Figure 1b).

The sampling site for Hg-contaminated sediments was chosen in the southernmost area of the Augusta Bay (Figure 1c), where high Hg contamination levels had been detected in previous monitoring campaigns (Figure 1d), and close to the southern Bay outlet, where the spread of contaminated sediments toward the open Mediterranean water was more likely [1].

Sampled sediments consisted of silt ($49.3 \pm 1.7\%$), clay ($40.8 \pm 3.0\%$), and sand ($9.9 \pm 1.7\%$). More than 100 kg of wet sediments were sampled during two sampling campaigns and used for both bench scale and mesocosm experiments.

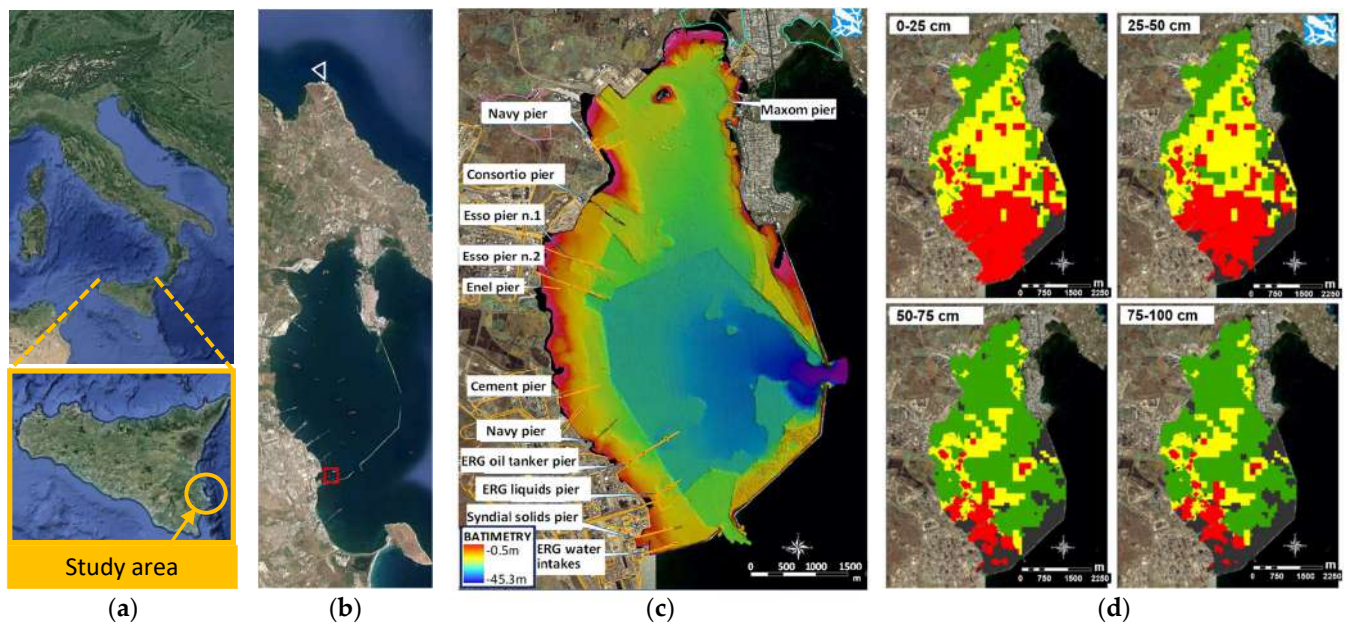


Figure 1. (a) Study area; (b) Location of the sediment sampling points: uncontaminated—white triangle, contaminated—red square; (c) location of various companies along the edge of the Augusta Bay and bathymetry of the Augusta Bay; (d) qualitative representation of the Hg contamination of the sediments at different depths from the bottom of the sea [43] (ICRAM 2008) (green cells = Hg < 1 mg/kg_{ss}; yellow cells = 1 mg/kg_{ss} < Hg < 5 mg/kg_{ss}; red cells = 5 mg/kg_{ss} < Hg < 500 mg/kg_{ss}).

2.2. Mesocosm Setup

All the experiments were carried out at the Mesocosm Facility at IAMC-CNR in Messina (Italy). Tanks measuring 150 × 150 × 150 cm (5 cm of free board) with a volume of approximately 3400 L were used in the experiment. The flow rate was 125 L/h, with a turnover of approximately 1 day [41]. Natural seawater was processed, as previously reported in Pirrone et al. [44]. A recirculation pump was operated within each mesocosm to simulate the effect of sediment resuspension—as induced by marine turbulence effects. The pump was turned on twice a day to cause the partial resuspension of the superficial layer of the sediment over the entire water column.

The experimental setup, outlined in Figure 2, included:

1. A white (W) mesocosm, with a bottom layer made of uncontaminated sediment (18 kg, with a thickness of ~6 mm), which was used as a control.
2. A black (B) mesocosm, with a bottom layer made of contaminated sediment (18 kg, with a thickness of ~6 mm) from Augusta, which was used to measure the effects of contamination on the *M. galloprovincialis* chosen as a sentinel.
3. A gray (G) mesocosm, with a bottom layer made of Augusta sediments previously treated by a soil-washing process, which was conceived to test the efficiency of the treatment process considered on *M. galloprovincialis*, as well as any undesired side-effects. The sediment-washing treatment was designed according to studies in the published literature [45] and previous experiments by the authors. In mesocosm G, 30 kg of the polluted sediments were previously treated with three cycles of a KI/I₂ soil-washing solution, which had been selected during bench-scale experiments and is explained in more detail later on in this paper. A total of 18 kg of treated sediments, with a thickness of ~6 mm, were disposed at the bottom of the gray mesocosm.

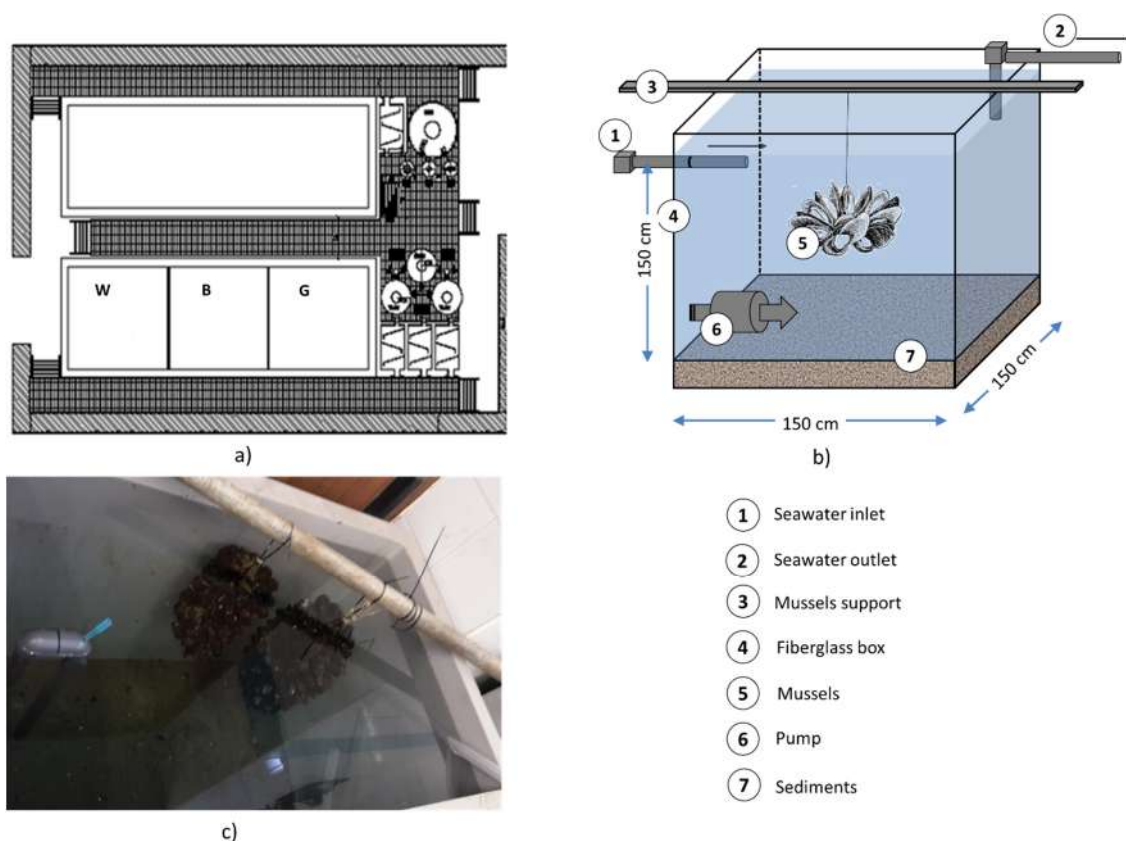


Figure 2. Mesocosm experiments: (a) Layout of the mesocosm facility at CNR-IAMC with the three mesocosms (white, gray, black); (b) Sketch of a single mesocosm. (c) Picture of the black mesocosm.

2.3. Chemical–Physical Parameters and Metal Measurements in Sediments and Water

Water samples from mesocosms were analyzed to determine the temperature and pH and DO, as reported in Caliani et al. [40] and Ancora et al. [41]. Water flowing into the mesocosms was interrupted during mixing and for a further 30 min to prevent the sediment from being lost from the systems. Sediment samples were analyzed using the EPA 3051A: 2007 and EPA 6020B:2014 analytical methods, which consist of acid microwave digestion and ICP-mass spectroscopy (ICP-MS NexION[®] 350D, Perkin Elmer, Waltham, MA, USA), respectively. Exhausted solutions and liquid fractions, produced by the acid digestion of the sediments, were analyzed according to EPA 6020B:2014 (ICP-mass spectroscopy).

2.4. Quality Control Hg Analysis

Briefly, all digested sediments were diluted with MilliQ[®] water to a final volume of 20 mL and filtered using nitrocellulose filters (0.45 μm). The test for Hg analysis was performed with an ICPMS Elan DRcE (ICP-MS NexION[®] 350D, Perkin Elmer, Waltham, MA, USA). Standards for instrument calibration were prepared using a multi-element certified reference solution ICP Standard (Merck), including the Hg. The system was calibrated using an external calibration; the calibration line was made up of 5 points of increasing concentration of Hg (by 0.0005 to 5 mg/kg), with a linear regression (R^2) of 0.9925. Analytical blanks and recovery samples were run in the same way as the real samples, and concentrations were determined using a standard solution prepared in the same acid matrix to validate the calibration. LOD of Hg was calculated as 0.00002 mg/g d.w.

2.5. Sequential Extraction Procedure

The sequential extraction procedure was carried out in triplicate (samples A, B and C) and consisted of seven steps, according to Orecchio et al. [46], as indicated in Table 1.

Table 1. Steps of the sequential extraction procedure.

Step	Fraction	Extraction
I	Water-soluble (Hg-w)	Solution: Distilled water Stirred for 20 min (250 rpm) Treated for 1 h at 95 °C
II	Soluble (Hg-h) or exchangeable human stomach acid	Solution: 1M of sodium acetate + 0.1 M di HCl Stirred for 1 h (250 rpm)
III	Carbonate Bound (Hg-CO ₃)	Solution: 1M of sodium acetate + acetic acid (pH = 5) Stirred for 4 h (250 rpm)
IV	Fe and Mn bound Hg (Hg-Me)	Solution: 0.04 M Hydroxylammonium chloride on 25% (v/v) acetic acid/water. Stirred for 20 min (250 rpm) Treated for 6 h at 95 °C
V	Organo-chelated (Hg-o)	Solution: 1 M potassium hydroxide Stirred for 18 h (250 rpm)
VI	Elemental Hg (Hg-e)	Solution: 12 M nitric acid Stirred for 18 h (250 rpm)
VII	Mercuric sulfide (Hg-s)	Acid digestion with aqua regia

2.6. Soil-Washing Tests

Soil-washing solutions were chosen from literature studies [45,47–49] on the extraction of heavy metals from soil and sediments, with particular attention to Hg contamination.

Four extraction agents were consequently tested on the Augusta Bay Hg-contaminated sediments:

- EDTA disodium salt (Ethylenedinitrilotetraacetic acid, disodium salt dihydrate, C₁₀H₁₂N₂Na₂O₈·2H₂O) 0.2 M solution;
- EDDS 1 M ([S,S]-ethylenediaminedisuccinic acid, C₁₀H₁₃N₂Na₃O₈) 1 M;
- Na₂S₂O₃ Sodium Thiosulfate 1 M;
- KI (potassium iodide) 0.2 M + I₂ (Iodine) 0.2 M.

All the leaching agents were of reagent grades.

First, two different sets of soil-washing lab-scale experiments were performed:

- (1) a single-step batch process (using the 4 leaching agents separately). This set was repeated twice in triplicate;
- (2) a three-step batch process, performed in triplicate, with the best-performing leaching agents as determined in the previous set of experiments.

The following procedure was used for each sediment sample: 2.00 g of sediment was weighed and put into a 50 mL vial. A vial was filled with 50 mL of the washing solution (solid/liquid ratio, S/L, equivalent to 1:25) and stirred for 2 h at a speed of 250 rpm. The vials were centrifuged at 4500 rpm for 10 min to separate suspended sediment from the exhausted solution. The liquid fraction was vacuum filtered using a 0.45 µm filter, and the eluate was acidified with HNO₃ (0.5–50 mL, 1:100 ratio) to maintain the extracted metals in the solution. The liquid fraction was refrigerated and kept in double-tap containers for subsequent analysis. The solid fraction was stored directly in the vial for subsequent analysis. The sediments used in the gray mesocosm were treated on a larger scale, according to the three-step soil-washing batch process, using an industrial mixer.

2.7. Histological Analysis

The mussel gills used for the histological assessment were fixed in 4% paraformaldehyde in a 0.1 M phosphate-buffered solution (PBS, pH 7.4) at 4 °C, dehydrated in a graded series of ethanol, and embedded in Paraplast (Bio-Optica, Milan, Italy). A total of 5 µm thick histological sections were cut using a rotary automatic microtome (Leica Microsystems,

Wetzlar, Germany), glass-slide mounted, and then stained with Hematoxylin/Eosin (Bio-Optica, Milan, Italy) to evaluate its morphological features. Observations were made on five fields of one section per sample using a 40× oil-immersion objective with a motorized Zeiss Axio Imager Z1 microscope (Carl Zeiss AG, Werk Gottingen, Germany) equipped with an AxioCam digital camera (Zeiss, Jena, Germany).

2.8. Immunohistochemical Analysis

The histological sections of the mussel gills were also used for the immunodetection of neurotransmission biomarkers by applying an indirect immunofluorescence method [50] for the localization of neurotransmitters involved in the serotonergic system, such as serotonin, or 5-hydroxytryptamine (5-HT) and its receptor (5-HT3R); and neural transmitters of cholinergic neurotransmission, such as acetylcholinesterase (AChE) and the enzyme choline acetyltransferase (ChAT). Briefly, sections were incubated for 1 h with a normal goat serum (NGS) in PBS (1:5) to block non-specific binding sites for immunoglobulins. The sections were then incubated overnight at 4 °C in a humid chamber with primary antisera, namely a mouse anti-5-HT antibody (Product No. M0758; Dako Cytomation, Milan, Italy), diluted 1:50; a rabbit anti-5-HT3R antibody (Product No. S1561; Sigma-Aldrich, St. Louis, MO, USA), diluted 1:100; a mouse anti-AChE antibody (Product No. MAB304; Chemicon International, Temecula, CA, USA), diluted 1:50; and a rabbit anti-ChAT antibody (Product No. AB6168; Abcam, Cambridge, UK), diluted 1:250. After rinsing the sections in PBS for 10 min, they were incubated for 2 h at room temperature with fluorescein isothiocyanate (FITC)-conjugated goat anti-rabbit IgG (Sigma) or tetramethylrhodamine isothiocyanate (TRITC)-conjugated goat anti-mouse IgG (Sigma), diluted 1:50. Positive controls were performed to label the specificity of each peptide by incubating sections with antiserum pre-absorbed by the respective antigen (10 and 100 g/mL). Pre-absorption procedures were carried out overnight at 4 °C. Negative controls, which involved substitution of the non-immune sera (without antibodies) with the primary antisera, were also performed. All the observations were made on five fields, considering one section per sample, and using a 40× oil-immersion objective with a motorized Zeiss Axio Imager Z1 epifluorescence microscope (Carl Zeiss AG, Werk Gottingen, Germany), equipped with an AxioCam digital camera (Zeiss, Jena, Germany). Images from the sections were taken using appropriate filters for the excitation of FITC (480/525 nm) and TRITC (515/590 nm) and then processed using AxioVision Release 4.5 software (Zeiss).

2.9. Enzymatic Analysis

Acetylcholinesterase (AChE) activity was measured in the gills of the mussels using the Ellman et al., colorimetric method [51], albeit with slight modifications. Briefly, thiocholine derivatives were hydrolyzed by acetylcholinesterase to yield thiocholine, which was then combined with 5,5-dithiobis-2-dinitrobenzoic acid (DTNB) to form the yellow 5-thio-2-nitrobenzoic acid anion, which absorbs to a great extent at 412 nm. AChE activity was expressed as mmol/min/mg.

2.10. Statistical Analysis

Statistical analyses of the immunohistochemical and enzymatic data were conducted with GraphPad software (Prism 5.0, San Diego, CA, USA). The results that were obtained were expressed as a mean ± standard deviation (SD). All data were first tested for normality by applying the Shapiro–Wilk test. One-way analysis of variance (ANOVA) was used to statistically analyze the data by applying the Mann–Whitney U test for immunohistochemical data, and Student's one-tailed *t*-test for enzymatic data. Data were considered statistically significant at $p < 0.05$.

3. Results

3.1. Water and Sediment Characterization in the Mesocosms

The water in the three mesocosms showed mean temperature values of 15.5–16.0 °C, with daily fluctuations of less than 1 °C. pH values were approximately constant, with a mean value of 7.9 ± 0.1 . Dissolved oxygen levels were similar in all three mesocosms with values of 7.95 ± 0.12 mg/L. Sediment samples were characterized in terms of their metal and hydrocarbon contents. The results of the sediment characterization are given in Table 2. Among the different metals, only the Hg concentration was above the intervention value proposed by ICRAM (2008) [43]. For this reason, Hg was the only target contaminant that was taken into account when assessing the soil-washing efficiency on these sediments.

Table 2. Sediment characterization of the Augusta (black) and Brucoli (white) samples and comparison with intervention limits.

Element	Black Sediment (mg kg ⁻¹)	White Sediment (mg kg ⁻¹)	Intervention Values [43] (mg kg ⁻¹)
Harmful heavy Metals			
As (mg/kg)	12.4 ± 1.9	10.09 ± 6.7	32
Cd (mg/kg)	0.197 ± 0.03	0.30 ± 0.16	1
Cr total (mg/kg)	27.7 ± 4.2	7.0 ± 0.3	150
Hg (mg/kg)	47.7 ± 7.2	0.04 ± 0.00	1
Ni (mg/kg)	12.6 ± 1.9	3.9 ± 0.1	63
Pb (mg/kg)	23 ± 3.5	5.55 ± 0.6	80
Cu (mg/kg)	60.3 ± 9.1	2.35 ± 0.06	75
Zn (mg/kg)	86 ± 13	10.1 ± 1.0	165
Hydrocarbons			
Light Hydrocarbons (C6-C12)	BDL (0.5)	BDL (0.5)	
Heavy hydrocarbons (C12-C20)	BDL (0.5)	BDL (0.5)	
Heavy hydrocarbons (C20-C30)	BDL (0.5)	BDL (0.5)	
Heavy hydrocarbons (C30-C40)	BDL (0.5)	BDL (0.5)	
Heavy hydrocarbons (C40-C50)	BDL (0.5)	BDL (0.5)	
Σ Heavy hydrocarbons (C12-C50)	BDL (0.5)	BDL (0.5)	

Note: BDL Below the detection limit.

3.2. Hg Sequential Extraction

3.2.1. Sample A

The standard sequential extraction procedure (SEP) conducted on sample A shows that more than 75% of the HgT in the sediments was extracted in step 6 (Figure 3), thus indicating that Hg has a highly stable phase and is trapped in a mineral lattice or bound to humic substances. Around 14% of the Hg was extracted in the seventh step (mercuric sulfide), in the same way as insoluble Hg forms such as cinnabar (HgS), m-HgS, HgSe, and HgAu. Less than 1% of the HgT was released in the first three steps, which involved more soluble and bioavailable forms.

3.2.2. Sample B

As in sample A, sample B had nearly 78% of HgT in the sediments extracted in step 6 (Figure 3). Around 9% of the Hg was extracted in the fifth step, as organo-chelated mercury. About 8% of the HgT was extracted in step 7, just like the insoluble Hg forms. Only 1% of the HgT was released in the first three steps (more soluble and bioavailable forms).

3.2.3. Sample C

The SEP of sample C shows that more than 74% of the HgT in the sediments was extracted in step 6 (Figure 3), thus confirming a highly stable phase of Hg trapped in a mineral lattice or bound to humic substances. Around 16% of the Hg was extracted in the fifth step as organo-chelated mercury. More than 9% was extracted in the seventh step,

just like such insoluble Hg forms as cinnabar (HgS), m-HgS, HgSe, and HgAu. Less than 1% of the HgT was released in the first three steps, that is, in a labile or human-stomach soluble form.

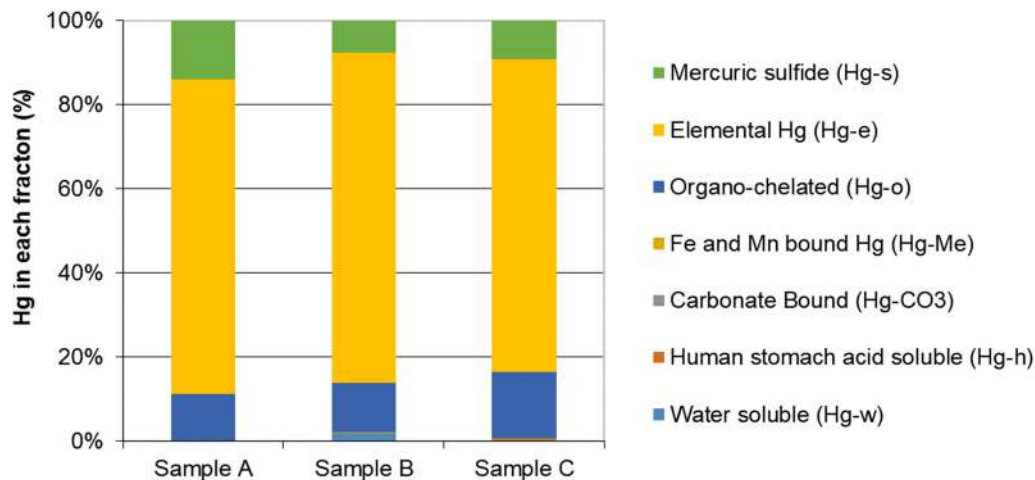


Figure 3. Results of the sequential extraction procedure (Hg expressed as percentage over the total Hg).

3.3. Soil Washing

The adopted soil-washing experiments are reported as a single-step batch process (two sets) and as a multi-step batch process. Both the lab test results and the ones obtained from the sediments used for the mesocosm set-up are indicated.

3.3.1. Single-Step Batch Process: First Set

The first batch leaching experiments indicated that, of the four tested solutions (Figure 4a), the iodide/iodine solution is the only one that was efficient in the removal of Hg from the examined sediments. On average, the solution extracted 88.9% of the Hg from aged sediments. On the other hand, the sodium thiosulfate solution only extracted 2% of Hg, and the EDDS and EDTA solutions did not extract any significant amounts of Hg (0.25% and 0.06% for EDTA and EDDS, respectively).

3.3.2. Single-Step Batch Process: Second Set

A second set of soil-washing experiments was performed, because of the highly heterogeneous efficiencies that were obtained from the first soil-washing batch test, using the same leaching solutions (EDTA, EDDS, Na₂S₂O₃ and KI/I₂) to validate the results of the first set of experiments on the specific sediment from the Augusta Bay. The second set of soil-washing experiments basically confirmed that the leaching efficiencies obtained from the first one (Figure 4b): EDTA and EDDS (efficiencies of 0.21% and 0.07%, respectively) were not fully effective in the removal of Hg; sodium thiosulfate did not have adequate removal capacity (3%) to implement a full-scale process; iodide/iodine (89.3%) could have the potential to be applied in industrial soil-washing processes aimed at the removal of Hg from sediments. These results prove that a high Hg extraction efficiency can be obtained by applying a suitably strong leaching agent to aged sediments, in agreement with the first conclusions obtained for the SEP procedure.

3.3.3. Single-Step Batch Process: Second Set

A second set of soil-washing experiments was performed, because of the highly heterogeneous efficiencies that were obtained from the first soil-washing batch test, using the same leaching solutions (EDTA, EDDS, Na₂S₂O₃ and KI/I₂) to validate the results of the first set of experiments on the specific sediment from the Augusta Bay. The second set of soil-washing experiments basically confirmed that the leaching efficiencies obtained from the first one (Figure 4b): EDTA and EDDS (efficiencies of 0.21% and 0.07%, respectively)

were not fully effective in the removal of HG; sodium thiosulfate did not have adequate removal capacity (3%) to implement a full-scale process; iodide/iodine (89.3%) could have the potential to be applied in industrial soil-washing processes aimed at the removal of Hg from sediments. These results prove that a high Hg extraction efficiency can be obtained by applying a suitably strong leaching agent to aged sediments, in agreement with the first conclusions obtained for the SEP procedure.

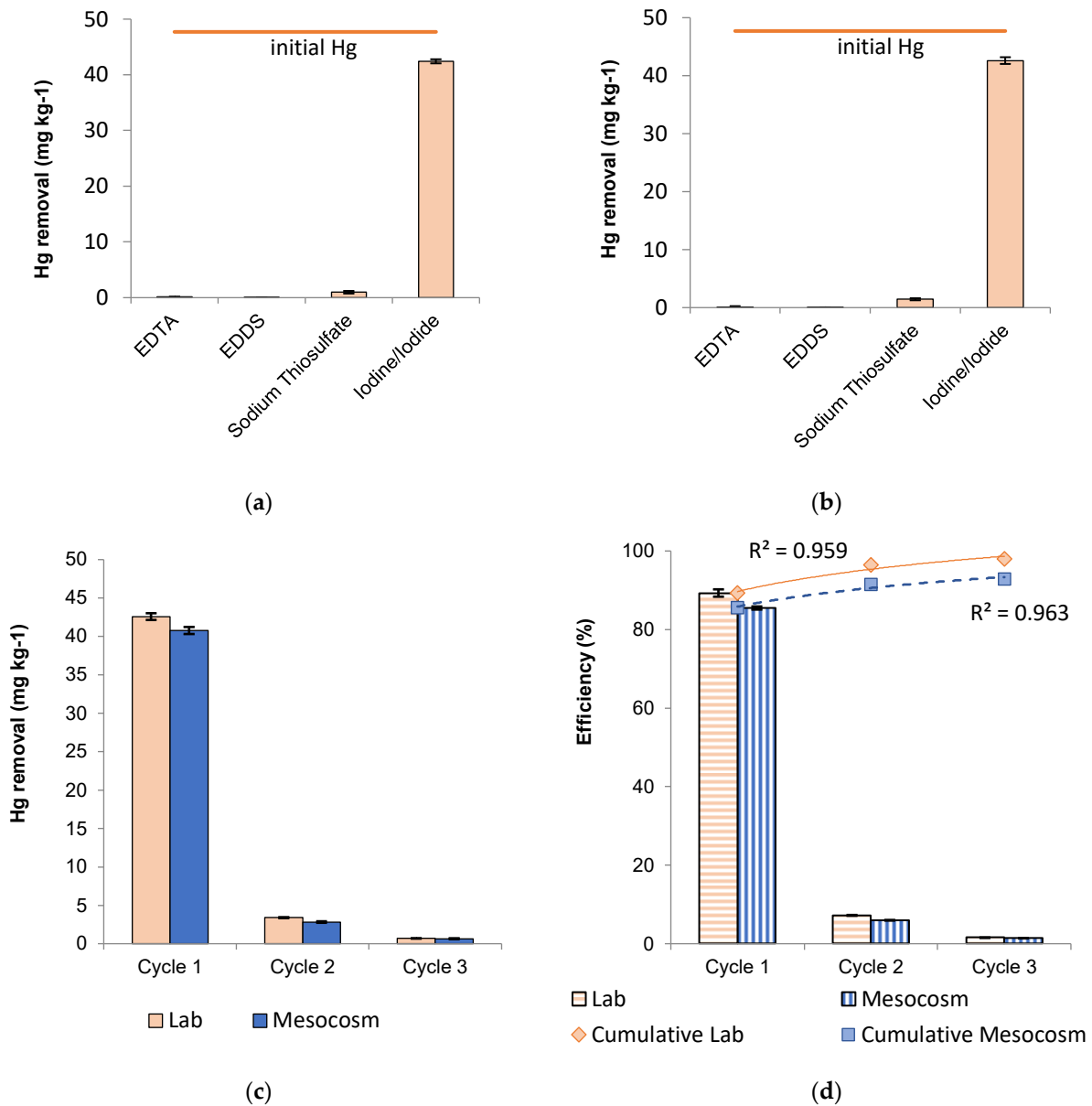


Figure 4. Results of the single-step soil-washing batch tests: (a) first set; (b) second set and of the multi-step soil-washing batch tests at the lab and mesocosm scales: (c) Hg mass removal; (d) Hg removal efficiency and cumulative expectation.

The iodide/iodine solution showed a mercury removal efficiency of 89.3% for the first soil-washing cycle, 67.1% for the second cycle, and 46.2% for the third cycle (Figure 4d). Each efficiency was calculated with regard to the initial concentration of Hg in the sediments at each step. The three-cycle lab process allowed an Hg concentration to be achieved in the sediments, which was below the intervention value (1 mg kg⁻¹), with an overall efficiency of 99%.

The overall quantity of sediments needed to implement mesocosm G (35 kg) was treated on the basis of the results of the lab-scale experiments. Achieved efficiencies (Figure 4d) were slightly lower than the ones obtained at the lab scale. The iodide/iodine solution showed a mercury removal efficiency of 85.5% for the first soil-washing cycle, 41.2% for the second cycle, and 16.7% for the third one. Each efficiency was calculated with regard to the initial Hg concentration of the sediment in each step. The overall efficiency of the three-step process was 92.9%. The three-cycle process achieved a residual concentration (3.41 mg kg^{-1}) that, unlike the results obtained with bench-scale experiments, was above the intervention value (1 mg kg^{-1}). This result was attributed to the need to process larger amounts of sediments and to the less energetic mixing carried out at the soil washing mesocosm with respect to the bench scale experiment.

Polynomial interpolation has been utilized to appraise the expected relationship between the number of washing cycles and achievable removal efficiency. It shows that, in the case of sediment treated at a larger mesocosm scale, a similar fourth cycle would probably remove only a marginal amount of Hg, thus making the sustainability of the increase in number of cycles with the same leaching agent concentration questionable. An increase in the strength of the leaching agent in subsequent steps or more energetic mixing conditions would probably help reduce residual concentration to below 1 mg kg^{-1} .

3.4. Histological Analysis

A normal morphology of mussel gill tissue (Figure 5a), consisting of parallel filaments whose whole surface is coated by cilia, was observed in the gills of *M. galloprovincialis* from mesocosm W. A relevant loss of cilia was noted in the gills of mussels from mesocosm B (Figure 5b), whereas a moderate alteration of cilia was revealed in the mussels from mesocosm G, together with a relevant presence of hemocytes in gill tissues (Figure 5c).

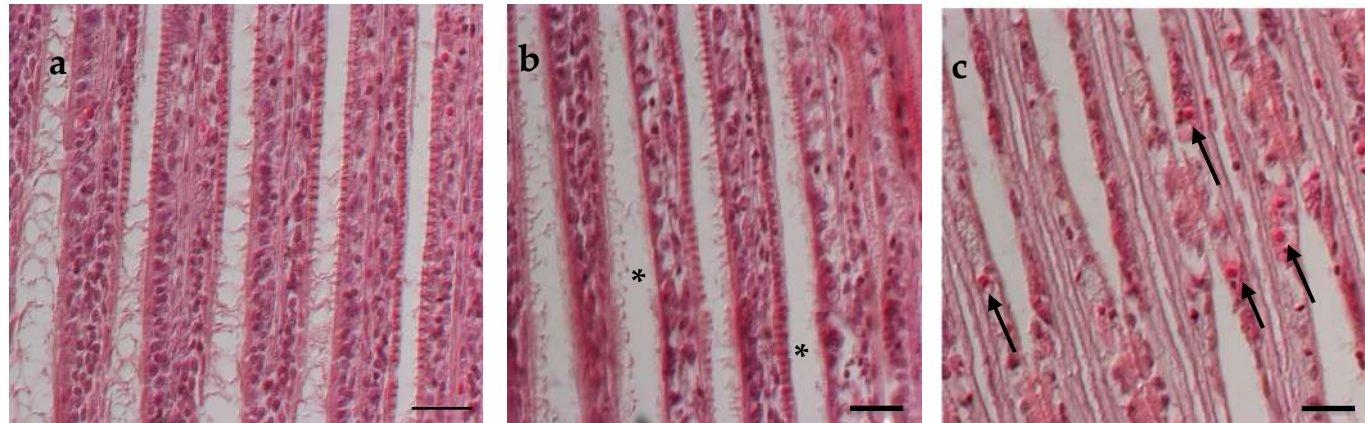


Figure 5. *M. galloprovincialis* gills stained with Hematoxylin and Eosin (H&E): (a) the white mesocosm, (b) the black mesocosm, (c) the gray mesocosm. (* indicates a loss of cilia, while arrows show hemocytes). Scale bars, 20 μm .

3.5. Immunohistochemical Analysis

As far as the serotonergic system is concerned, the gills of the mussels from mesocosm W showed high cellular immunopositivity for 5-HT (Figure 6(a1)) and a low expression for 5-HT₃R (Figure 6(b1)). A reduction in immunopositivity was observed in mesocosm B for serotonin (Figure 6(a2)), with a concomitant increase in the signal of the receptor at a gill fiber level (Figure 6(b2)). Moreover, a moderate increase in 5-HT immunopositivity was revealed in both the cells and fibers of gills of mussels from mesocosm G (Figure 6(a3)), compared to mesocosm B, while the receptor was mainly localized along the fibers and in the hemocytes (Figure 6(c3)). Quantification and statistics of 5-HT (Figure S1) and 5-HT₃R (Figure S2) immunopositive cells detected in the gills of the mussels from the three meso-cosms are reported in the Supplementary Materials.

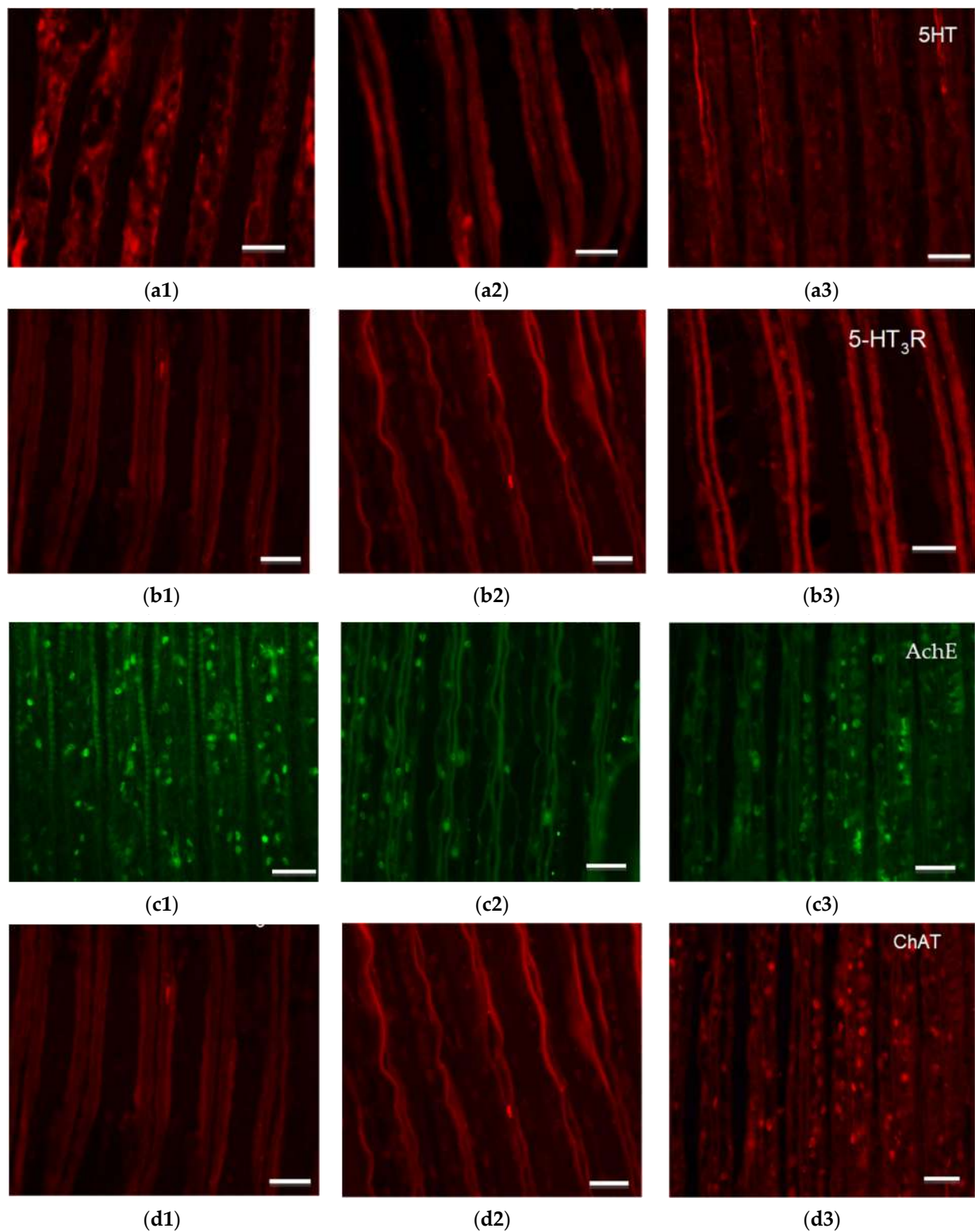


Figure 6. Immunohistochemical labeling of 5-HT in the gills of the mussels from: (a1) the white mesocosm, (a2) the black mesocosm, and (a3) the gray mesocosm; Immunohistochemical labeling of 5-HT₃R in the gills of the mussels from (b1) the white mesocosm, (b2) the black mesocosm, and (b3) the gray mesocosm; Immunohistochemical labeling of AChE in the gills of the mussels from (c1) the white mesocosm, (c2) the black mesocosm, and (c3) the gray mesocosm; Immunohistochemical labeling of ChAT in the gills of the mussels from (d1) the white mesocosm, (d2) the black mesocosm, and (d3) the gray mesocosm. Scale bars, 20 μ m.

As for the cholinergic system, AChE and ChAT showed good immunopositivity in the gill cells of the control mussels from mesocosm W (Figure 6(c1,d1)). Low cellular immunopositivity of AChE and ChAT was observed in mesocosm B, with a higher signal in the fibers (Figure 6(c2,d2)). The immunopositivity of both enzymes increased in mesocosm G, compared with mesocosm B, and was mainly expressed in the cells (Figure 6(c3,d3)). Quantification and statistics of AChE (Figure S3) and ChAT (Figure S4) immunopositive cells detected in the gills of the mussels from the three mesocosms are reported in the Supplementary Materials.

3.6. Enzymatic Analysis

A significant reduction of about 20% of AChE activity was revealed, through a comparison of enzymatic activity in the three different mesocosms, only in the gills of the mussels exposed to the natural polluted sediments in mesocosm B (data statistically significant). The enzymatic activity of AChE was not inhibited in mesocosm G where the sediments were treated by soil washing, as its level was almost equivalent to that recorded in mesocosm W (Figure 7).

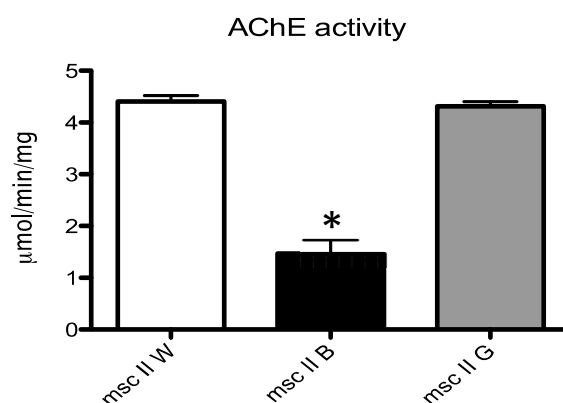


Figure 7. AChE activity measured in the gills of the mussels from (msc II W) the white mesocosm, (msc II B) the black mesocosm, and (msc II G) the gray mesocosm. Results are reported as mean and standard deviation (SD). Significant differences ($p < 0.05$) between groups are indicated by an asterisk.

3.7. Hg Removal Efficiency

Hg Removal efficiencies, as evaluated in this study, were compared with other literature data evaluating leaching agents and Hg initial concentration, as reported in Table 3.

Table 3. Comparison of different Hg removal efficiencies as functions of the leaching agent and the initial Hg content.

Ref.	Process	Reagent	Hg Initial Concentration (mg/g)	Hg Removal Efficiency (%)
[47]	Column	0.1 M KI + 0.5 M HCl	113.5	76
	Batch	0.1 M KI + 0.5 M HCl	47.1	99
[48]	Batch	0.2 M I ₂ + 0.4 M KI	35.0	98
	Batch	0.1 M KI	6.1	28
[45]	Batch	1 M Na ₂ S ₂ O ₃	6.1	37
	Column	0.1 M KI	6.1	35
[49]	Three-step batch	H ₂ O ₂ , Na ₂ S ₂ O ₃ , Na ₂ S	2.1	87
This study	Single-step batch	EDTA 0.2 M	47.7	0.2

Table 3. Cont.

Ref.	Process	Reagent	Hg Initial Concentration (mg/g)	Hg Removal Efficiency (%)
This study	Single-step batch	EDDS 0.1 M	47.7	0.7
This study	Single-step batch	Na ₂ S ₂ O ₃	47.7	2.5
This study	Single-step batch	KI 0.2 M + I ₂ 0.2 M.	47.7	89.3–85.5 *
This study	Double-step batch	KI 0.2 M + I ₂ 0.2 M.	47.7	96.4–91.5 *
This study	Three-step batch	KI 0.2 M + I ₂ 0.2 M.	47.7	98.0–93.0 *

* lab (first value), mesocosm (second value).

4. Discussion

As already mentioned, Hg contamination in the Augusta Bay is caused by discharges from a chlor-alkali plant, based on Hg-cell technology, which was in operation from 1958 to 2003. During that period, it was legally permitted to “wash” the Hg-cell with seawater, and this led to an estimated discharge of over 500 tons of Hg into the sea [52]. Because of the historical origin of this Hg contamination, it is possible to refer to such contaminated sediments as being “aged”. This aspect has significant implications in terms of sequential extraction results, as well as in terms of the main expected mechanism of mussel contamination.

The toxicity and bioavailability of mercury in sediments depend above all on the site-specific distribution of its forms and their interaction with the sediment matrix under aqueous conditions. Sediment pore water, which usually contains high concentrations of mercury, could readily release mercury into overlying water [53]. Certain activities, such as dredging and shipping, as well as natural occurrences, such as storms and tides, could also remobilize mercury from the sediments [54]. Bloom and Loasorsa [55] conducted a laboratory experiment in which they mimicked ocean dredging, and they reported that about 5% of MeHg and less than 1% of total mercury was released from contaminated sediments during the dredging simulation. SEP results can help to identify the main binding sites and phase associations of Hg when assessing the risk for humans and the environment.

The sequential extraction procedure showed that Hg is strongly bound to sediments, since very aggressive reagents were necessary for its extraction from the solid matrix. Hg is mostly present in the matrix in the form of elemental mercury (60%). These results are fully in agreement with those obtained from other SEP studies carried out on sediments from the Augusta Bay [46,56].

The results of the fractionation analysis were used to establish the most suitable agents to use as leaching solutions to remove aged Hg-polluted sediments, like those from the Augusta coastal area. Table 3 shows a comparison of the different Hg removal efficiencies as functions of the leaching process, the leaching agent, and the initial content of Hg in the treated matrix.

The poor results obtained with EDTA and EDDS are not surprising, as Mercury is a class B element with a very high covalence index and no affinity for oxygenated groups (involving carboxylic and alcoholic or phenolic functional groups), such as those present in EDTA or EDDS. However, these two chelating agents were tested here to provide the local Harbour Authority with direct and clear information of the inadequacy in the use of these compounds for such applications. For the chelation of Hg, the -SH group shows an enormous affinity, as do amines and polyphenols. Examples of these chelators are the recurrently used Dimercaprol (2,3-Dimercaptopropanol), also called BAL (British anti-Lewisite), and the usual medication to treat poisoning from Hg. Other chelators for Hg are Penicillamine, Dimercaptosuccinic acid, etc. Chelators containing thiol, amines, or polyphenols groups could improve results obtained by an iodide/iodine solution.

The results of this study also suggest that, in the case of the Augusta Bay, the main contamination path could now be the simple resuspension of aged sediments induced by marine turbulence or by anthropic activities that cause the local fauna to directly “ingest”

contaminated particles. Since Hg is predominantly present in a very stable form, the risk of its dissolution in the water is more limited. For this reason, a more holistic approach is needed to assess the effect of potential Hg contamination.

The use of a multi-biomarker approach to perform a comprehensive evaluation of the biological responses elicited by *M. galloprovincialis* mussels challenged by petrochemical pollution has already been employed successfully [44,57,58]. It was documented that the histomorphological alterations of biological tissues represent a signal of damage and also of the functional integrity of the tissues [58,59]. In this study, the gills of mussels from mesocosm B exhibited severe histological damage, as well as an important loss of cilia, whereas only moderate alterations were observed in the branchial epithelium of the mussels from mesocosm G, even though the presence of hemocytes was evident. The cilia of marine mollusks are actively involved in numerous gill functions, such as nutrient uptake and gas exchange, while hemocytes have a complex cell-signaling network that has a high homology with that of vertebrates, which allows them to modulate their own functions [60,61]. The observation of hemocytes, a sign of inflammation, in the gills of mussels from mesocosm G from treated sediments is due to the presence of residual mercury. In fact, soil washing was able to reduce metal concentrations, but mercury levels remained above allowed limits (Ministerial Decree No. 260/2010; Dutch Sediment Quality Guidelines, SQGs). The residual presence of Hg in treated sediments might have been able to trigger cytotoxic and inflammatory responses in the branchial tissue of the mussels.

In order to evaluate the neurotoxic potential of the residual contaminant, which is still present—albeit to a lesser extent—a battery of biomarkers that are indicative of neuronal perturbations, mainly related to the serotonergic and cholinergic neurotransmission system that regulates the movement and beating of gill cilia [62–64], was also assessed in treated sediments. As far as the serotonergic system is concerned, the immunopositivity to serotonin in the gills of mussels from mesocosm G was found to be lower than in mesocosm W but moderately higher than in the mussels from mesocosm B. Reduction in serotonin, as observed in mesocosm B, was comparable with data reported about the gills of mussels exposed to complex pollution in the field [58,59]. The increased immunopositivity of serotonin recorded in mesocosm G indicates that the condition present in the mesocosm with treated sediments is somewhat similar to the control environment represented by mesocosm W. As expected, evaluation of the 5-HT receptor, by means of the immunohistochemical assay in mesocosm B, showed an increase in serotonin receptor immunopositivity compared to that recorded in mesocosm W. This result is an adaptive response that is mediated, in the gills, by paracrine signaling activities that are aimed at recovering the regular physiological activity of the branchial epithelium [58,59,63]. Reduction in 5-HT₃R immunopositivity in mesocosm G with the treated sediments is worth noting, and it is similar to the response observed in mesocosm W, thus suggesting a tendency for mussels to recover a healthy condition.

The cholinergic system was also investigated with the aim of obtaining more complete insights into the neurotoxic potential of any petrochemical pollutants still present in sediments after treatment. The cholinergic system is responsible for the physiological functioning of the efferent nervous system [64]. The choline acetyltransferase enzyme (ChAT) is responsible for synthesis of the neurotransmitter acetylcholine into the cytoplasm of cholinergic neurons, whereas the acetylcholinesterase enzyme (AChE) catalyzes the breakdown of acetylcholine into choline and acetate within cholinergic synapses and neuromuscular junctions [65]. The immunopositivity of the two enzymes in the gills of mussels from mesocosm B was found to be lower than that recorded in the mussels from mesocosm W (control) and mesocosm G (treated sediments). This data were also confirmed through the measurement of the enzymatic activity of AChE in mussel gills, which was significantly reduced in the mussels from mesocosm B, compared to those in mesocosms W and G. The concomitance of the inhibition of both AChE and ChAT is a clear sign of the severe compromising of the cholinergic system, since no adaptive compensatory responses were elicited by the mussels, thereby resulting in important repercussions for the ciliary

function and also for the filtering activity of mussel gills. Similar data had previously been documented in a field study with mussels caged for 60 days in a coastal marine area greatly affected by multi-contaminant (i.e., hydrocarbon and Hg) pollution [58].

5. Conclusions

The results of bench-scale washing tests indicated the Hg removal efficiency that is achievable through a multi-step process. Overall removal efficiencies were 99% and 93% at the lab and meso scale, respectively, when the most effective extractive agent (iodide) was used. Chelators containing thiol, amines, or polyphenols groups could improve the results obtained by an iodide/iodine solution.

Regardless of the experimental efficiency obtained and the specific removal process adopted here, the main aim of the work is to propose an innovative approach that is aimed at preventively assessing the environmental (positive) impact of a remediation/treatment process, not only through conventional chemical measurements (i.e., the achieved reduction in pollutant concentrations in the treated matrix—regardless of how it is performed and reported) but also through a simultaneous and direct measurement of the remediation strategy effects on a target biological community. Although we have focused on the soil washing of Hg-contaminated sediments (i.e., removing–treating–reallocating the sediments) as a potential decontamination strategy in this paper, the proposed approach could be applied to several other processes through a comparative approach. In other words, when restoring a contaminated environment or reducing pollutant discharge (e.g., industrial wastewater discharge), the use of mesocosms could help to preventively address the selection of the most efficient process by simulating—at a significant but still controlled scale—the marine environment and its biological response. By comparing the effects of both the untreated and treated matrix (i.e., the sediments) on the same sentinels, the proposed approach appears to be much more effective than using only traditional chemical measurements of the efficiency of treatment, and thus, a more direct and holistic picture of the final environmental effect of the restoration can be attained. When referring to a controlled system, any potential field (site-specific) interferences are prevented, and only the effects of the proposed treatment can thus be “read”.

The proposed approach that can be applied to any kind of remediation/treatment action in any part of the world could help stakeholders to allocate funds to the best strategy by selecting, at an early stage, the most efficient cleaning action from a more holistic and broader perspective.

Supplementary Materials: The following supporting information can be downloaded at <https://www.mdpi.com/article/10.3390/w15183258/s1>. Figure S1: Quantification of 5-HT immunopositive cells in the gills of mussels from the three mesocosms; Figure S2: Quantification of 5-HT3R immunopositive cells in the gills of mussels from the three mesocosms; Figure S3: Quantification of AChE immunopositive cells in the gills of mussels from the three mesocosms; Figure S4: Quantification of ChAT immunopositive cells in the gills of mussels from the three mesocosms.

Author Contributions: Conceptualization, G.M., S.C., M.M. and R.G.; Methodology, G.M., S.C., M.M., T.C., G.D.M., R.G., M.S., A.L., P.V. and D.F.; Validation, A.L., T.C., G.D.M., M.S., P.V. and D.F.; Formal Analysis, T.C., G.D.M. and R.G.; Investigation, G.M., S.C., M.M. and T.C.; Resources, G.M., S.C. and M.M.; Writing—Original Draft Preparation, G.M., A.L., T.C., M.M. and D.F.; Writing—Review & Editing, G.M., A.L., S.C., G.D.M., T.C., M.M., R.G., M.S., P.V. and D.F.; Visualization, G.M., A.L., S.C., T.C., M.M., R.G., G.D.M., M.S., P.V. and D.F.; Supervision, G.M., S.C. and D.F.; Project Administration, G.M., S.C. and A.L.; Funding Acquisition, G.M., S.C., M.M. and M.S. All authors have read and agreed to the published version of the manuscript.

Funding: This work was supported by the Italian National Interest Research Project (PRIN 2010-2011, prot. 2010ARBLT7_001/008).

Data Availability Statement: The data will be available upon request to authors.

Conflicts of Interest: The authors declare no conflict of interest.

References

1. Sprovieri, M.; Oliveri, E.; Di Leonardo, R.; Romano, E.; Ausili, A.; Gabellini, M.; Barra, M.; Tranchida, G.; Bellanca, A.; Neri, R.; et al. The key role played by the Augusta basin (southern Italy) in the mercury contamination of the Mediterranean Sea. *J. Environ. Monit.* **2011**, *13*, 1753–1760. [CrossRef] [PubMed]
2. Law No. 319 of 10th May 1976 ‘Water Protection against Pollution’ (Merli Law). Available online: <https://www.gazzettaufficiale.it/eli/id/1976/05/29/076U0319/sg> (accessed on 21 November 2021).
3. Ausili, A.; Gabellini, M.; Cammarata, G.; Fattorini, D.; Benedetti, M.; Pisanelli, B.; Gorbi, S.; Regoli, F. Ecotoxicological and Human Health Risk in a Petrochemical District of Southern Italy. *Mar. Environ. Res.* **2008**, *66*, 215–217. [CrossRef]
4. Feng, C.; Pedrero, Z.; Lima, L.; Olivares, S.; de La Rosa, D.; Berail, S.; Tessier, E.; Pannier, F.; Amouroux, D. Assessment of Hg contamination by a Chlor-Alkali Plant in riverine and coastal sites combining Hg speciation and isotopic signature (Sagua la Grande River, Cuba). *J. Hazard. Mater.* **2019**, *371*, 558–565. [CrossRef]
5. Wang, C.; Song, Z.; Li, Z.; Zhu, W.; Li, P.; Feng, X. Mercury speciation and mobility in salt slurry and soils from an abandoned chlor-alkali plant, Southwest China. *Sci. Total Environ.* **2019**, *652*, 900–906. [CrossRef] [PubMed]
6. Guney, M.; Akimzhanova, Z.; Kumisbek, A.; Beisova, K.; Kismelyeva, S.; Satayeva, A.; Inglezakis, V.; Karaca, F. Mercury (Hg) Contaminated Sites in Kazakhstan: Review of Current Cases and Site Remediation Responses. *Int. J. Environ. Res. Public Health* **2020**, *17*, 8936. [CrossRef]
7. Salvagio Manta, D.; Bonsignore, M.; Oliveri, E.; Barra, M.; Tranchida, G.; Giaramita, L.; Mazzola, S.; Sprovieri, M. Fluxes and the Mass Balance of Mercury in Augusta Bay (Sicily, Southern Italy). *Estuar. Coast. Shelf Sci.* **2016**, *181*, 134–143. [CrossRef]
8. Di Leonardo, R.; Adelfio, G.; Bellanca, A.; Chiodi, M.; Mazzola, S. Analysis and Assessment of Trace Element Contamination in Offshore Sediments of the Augusta Bay (SE Sicily): A Multivariate Statistical Approach Based on Canonical Correlation Analysis and Mixture Density Estimation Approach. *J. Sea Res.* **2014**, *85*, 428–442. [CrossRef]
9. Harding, G.; Dalziel, J.; Vass, P. Bioaccumulation of methylmercury within the marine food web of the outer Bay of Fundy, Gulf of Maine. *PLoS ONE* **2018**, *13*, 0197220. [CrossRef]
10. Al-Sulaiti, M.M.; Soubra, L.; Al-Ghouthi, M.A. The Causes and Effects of Mercury and Methylmercury Contamination in the Marine Environment: A Review. *Curr. Pollut. Rep.* **2022**, *8*, 249–272. [CrossRef]
11. Eckley, C.S.; Gilmour, C.C.; Janssen, S.; Luxton, T.P.; Randall, P.M.; Whalin, L.; Austin, C. The assessment and remediation of mercury contaminated sites: A review of current approaches. *Sci. Total Environ.* **2020**, *707*, 136031. [CrossRef]
12. Randall, P.M.; Chattopadhyay, S. Mercury Contaminated Sediment Sites—An Evaluation of Remedial Options. *Environ. Res.* **2013**, *125*, 131–149. [CrossRef]
13. Schultz, T.; Korhonen, P.; Virtanen, M. A mercury model used for assessment of dredging impacts. *Water Air Soil Pollut.* **1995**, *80*, 1171–1180. [CrossRef]
14. Garbaciak, S.; Spadaro, P.; Thornburg, T.; Fox, R. Sequential risk mitigation and the role of natural recovery in contaminated sediment projects. *Water Sci. Technol.* **1998**, *37*, 331–336. [CrossRef]
15. Ebinghaus, R.; Turner, R.R.; de Lacerda, L.D.; Vasiliev, O.; Salomons, W. *Mercury Contaminated Sites: Characterization, Risk Assessment and Remediation*; Springer: Berlin/Heidelberg, Germany, 1998.
16. Yan, F.; Reible, D. Electro-bioremediation of contaminated sediment by electrode enhanced capping. *J. Environ. Manag.* **2015**, *155*, 154–161. [CrossRef]
17. Evangelou, M.W.H.; Ebel, M.; Schaeffer, A. Chelate Assisted Phytoextraction of Heavy Metals from Soil. Effect, Mechanism, Toxicity, and Fate of Chelating Agents. *Chemosphere* **2007**, *68*, 989–1003. [CrossRef]
18. Lesa, B.; Aneggi, E.; Rossi, G.; Comuzzi, C.; Goi, D. Bench-scale tests on ultrasound-assisted acid washing and thermal desorption of mercury from dredging sludge and other solid matrices. *J. Hazard. Mater.* **2009**, *171*, 647–653. [CrossRef] [PubMed]
19. Luciano, A.; Viotti, P.; Torretta, V.; Mancini, G. Numerical approach to modelling pulse-mode soil flushing on a Pb-contaminated soil. *J. Soils Sediments* **2013**, *13*, 43–55. [CrossRef]
20. Satyro, S.; Race, M.; Marotta, R.; Dezotti, M.; Spasiano, D.; Mancini, G.; Fabbricino, M. Simulated Solar Photocatalytic Processes for the Simultaneous Removal of EDDS, Cu(II), Fe(III) and Zn(II) in Synthetic and Real Contaminated Soil Washing Solutions. *J. Environ. Chem. Eng.* **2014**, *2*, 1969–1979. [CrossRef]
21. Xu, J.; Bravo, A.G.; Lagerkvist, A.; Bertilsson, S.; Sjöblom, R.; Kumpiene, J. Sources and remediation techniques for mercury contaminated soil. *Environ. Int.* **2015**, *74*, 42–53. [CrossRef] [PubMed]
22. Han, C.; Wang, H.; Xie, F.; Wang, W.; Zhang, T.; Dreisinger, D. Feasibility study on the use of thiosulfate to remediate mercury-contaminated soil. *Env. Environ. Technol.* **2019**, *40*, 813–821. [CrossRef] [PubMed]
23. Taube, F.; Pommer, L.; Larsson, T.; Shchukarev, A.; Nordin, A. Soil Remediation—Mercury Speciation in Soil and Vapor Phase During Thermal Treatment. *Water Air Soil Pollut.* **2008**, *193*, 155–163. [CrossRef]
24. Issaro, N.; Abi-Ghanem, C.; Bermond, A. Fractionation studies of mercury in soils and sediments: A review of the chemical reagents used for mercury extraction. *Anal. Chim. Acta* **2009**, *631*, 1–12. [CrossRef] [PubMed]
25. Cappello, S.; Genovese, M.; Denaro, R.; Santisi, S.; Volta, A.; Bonsignore, M.; Mancini, G.; Giuliano, L.; Genovese, L.; Yakimov, M.M. Quick Stimulation of *Alcanivorax* Sp. By Bioemulsificant EPS2003 on Microcosm Oil Spill Simulation. *Braz. J. Microbiol.* **2015**, *45*, 1317–1323. [CrossRef]
26. Mancini, G.; Cappello, S.; Yakimov, M.M.; Polizzi, A.; Torregrossa, M. Biological approaches to the treatment of saline oily waste(waters) originated from marine transportation. *Chem. Eng. Trans.* **2012**, *27*, 37–42.

27. Mancini, G.; Lanciotti, E.; Bruno, M. Chemical-physical and biological treatment of high salinity wastewaters contaminated by oily xenobiotic compounds. *Chem. Eng. Trans.* **2010**, *20*, 271–278.
28. Adel, M.; Copat, C.; Oliveri Conti, G.; Sakhaie, F.; Hashemi, Z.; Mancini, G.; Cristaldi, A.; Ferrante, M. Trace elements in the muscle tissue of *Hemiculter leucisculus* and *Abramis brama orientalis* from the Anzali International wetland, south-west of Caspian Sea: An exposure risk assessment. *Mar. Pollut. Bull.* **2022**, *180*, 113756. [[CrossRef](#)]
29. Copat, C.; Rizzo, M.; Zuccaro AGrasso, A.; Zuccarello, P.; Fiore, M.; Mancini, G.; Ferrante, M. Metals/Metalloids and Oxidative Status Markers in Saltwater Fish from the Ionic Coast of Sicily, Mediterranean Sea. *Int. J. Environ. Res.* **2020**, *14*, 15–27. [[CrossRef](#)]
30. Scalici, M.; Traversetti, L.; Spani, F.; Malafoglia, V.; Colamartino, M.; Persichini, T.; Cappello, S.; Mancini, G.; Guerriero, G.; Colasanti, M. Shell fluctuating asymmetry in the sea-dwelling benthic bivalve *Mytilus galloprovincialis* (Lamarck, 1819) as morphological markers to detect environmental chemical contamination. *Ecotoxicology* **2017**, *26*, 396–404. [[CrossRef](#)]
31. Santisi, S.; Cappello, S.; Catalfamo, M.; Mancini, G.; Hassanshahian, M.; Genovese, L.; Giuliano, L.; Yakimov, M.M. Biodegradation of crude oil by individual bacterial strains and a mixed bacterial consortium. *Braz. J. Microbiol.* **2015**, *46*, 377–387. [[CrossRef](#)]
32. Santisi, S.; Catalfamo, M.; Bonsignore, M.; Gentile, G.; Di Salvo, E.; Genovese, M.; Mahjoubi, M.; Cherif, A.; Mancini, G.; Hassanshahian, M.; et al. Biodegradation ability of two selected microbial autochthonous consortia from a chronically polluted marine coastal area (Priolo Gargallo, Italy). *J. Appl. Microbiol.* **2019**, *127*, 618–629. [[CrossRef](#)]
33. Giacoletti, A.; Cappello, S.; Mancini, G.; Mangano, M.C.; Sarà, G. Predicting the effectiveness of oil recovery strategies in the marine polluted environment. *J. Environ. Manag.* **2018**, *223*, 749–757. [[CrossRef](#)]
34. Mancini, G.; Panzica, M.; Fino, D.; Cappello, S.; Yakimov, M.M.; Luciano, A. Feasibility of treating emulsified oily and salty wastewaters through coagulation and bio-regenerated GAC filtration. *J. Environ. Manag.* **2017**, *203*, 817–824. [[CrossRef](#)] [[PubMed](#)]
35. Cappello, S.; Volta, A.; Santisi, S.; Morici, C.; Mancini, G.; Quatrini, P.; Genovese, M.; Yakimov, M.M.; Torregrossa, M. Oil-degrading bacteria from a membrane bioreactor (BF-MBR) system for treatment of saline oily waste: Isolation, identification and characterization of the biotechnological potential. *Int. Biodeterior. Biodegrad.* **2016**, *110*, 235–244. [[CrossRef](#)]
36. Cappello, S.; Calogero, R.; Santisi, S.; Genovese, M.; Denaro, R.; Genovese, L.; Giuliano, L.; Mancini, G.; Yakimov, M.M. Bioremediation of oil polluted marine sediments: A bio-engineering treatment. *Int. Microbiol.* **2015**, *18*, 127–134. [[PubMed](#)]
37. Fasulo, S.; Guerriero, G.; Cappello, S.; Colasanti, M.; Schettino, T.; Leonzio, C.; Mancini, G.; Gornati, R. The “SYSTEMS BIOLOGY” in the study of xenobiotic effects on marine organisms for evaluation of the environmental health status: Biotechnological applications for potential recovery strategies. *Rev. Environ. Sci. Biotechnol.* **2015**, *14*, 339–345. [[CrossRef](#)]
38. Caricato, R.; Giordano, M.E.; Schettino, T.; Maisano, M.; Mauceri, A.; Giannetto, A.; Cappello, T.; Parrino, V.; Ancora, S.; Caliani, I.; et al. Carbonic anhydrase integrated into a multimarker approach for the detection of the stress status induced by pollution exposure in *Mytilus galloprovincialis*: A field case study. *Sci. Total Environ.* **2019**, *690*, 140–150. [[CrossRef](#)]
39. Rossi, F.; Palombella, S.; Pirrone, C.; Mancini, G.; Bernardini, G.; Gornati, R. Evaluation of Tissue Morphology and Gene Expression as Biomarkers of Pollution in Mussel *Mytilus Galloprovincialis* Caging Experiment. *Aquat. Toxicol.* **2016**, *181*, 57–66. [[CrossRef](#)]
40. Caliani, I.; De Marco, G.; Cappello, T.; Giannetto, A.; Mancini, G.; Ancora, S.; Maisano, M.; Parrino, V.; Cappello, S.; Bianchi, N.; et al. Assessment of the effectiveness of a novel BioFilm-Membrane BioReactor oil-polluted wastewater treatment technology by applying biomarkers in the mussel *Mytilus galloprovincialis*. *Aquat. Toxicol.* **2022**, *243*, 106059. [[CrossRef](#)]
41. Ancora, S.; Rossi, F.; Borgese, M.; Pirrone, C.; Caliani, I.; Cappello, S.; Mancini, G.; Bianchi, N.; Leonzio, C.; Bernardini, G.; et al. Assessing the Effect of Contaminated and Restored Marine Sediments in Different Experimental Mesocosms Using an Integrated Approach and *Mytilus galloprovincialis* as a Model. *Mar. Biotechnol.* **2020**, *22*, 411–422. [[CrossRef](#)]
42. Gornati, R.; Maisano, M.; Pirrone, C.; Cappello, T.; Rossi, F.; Borgese, M.; Giannetto, A.; Cappello, S.; Mancini, G.; Bernardini, G.; et al. Mesocosm System to Evaluate BF-MBR Efficacy in Mitigating Oily Wastewater Discharges: An Integrated Study on *Mytilus galloprovincialis*. *Mar. Biotechnol.* **2019**, *21*, 773–790. [[CrossRef](#)]
43. ICRAM. *Progetto Preliminare di Bonifica dei Fondali Della Rada di Augusta nel Sito di Interesse Nazionale di Priolo—Elaborazione Definitiva*; BoI-Pr-SI-PR-Rada di Augusta-03.22 (182p); Istituto Centrale Per La Ricerca Scientifica E Tecnologica Applicata Al Mare: Rome, Italy, 2008.
44. Pirrone, C.; Rossi, F.; Cappello, S.; Borgese, M.; Mancini, G.; Bernardini, G.; Gornati, R. Evaluation of biomarkers in *Mytilus galloprovincialis* as an integrated measure of biofilm-membrane bioreactor (BF-MBR) system efficiency in mitigating the impact of oily wastewater discharge to marine environment: A microcosm approach. *Aquat. Toxicol.* **2018**, *198*, 49–62. [[CrossRef](#)]
45. Subirés-Muñoz, J.D.; García-Rubio, A.; Vereda-Alonso, C.; Gómez-Lahoz, C.; Rodríguez-Maroto, J.M.; García-Herruzo, F.; Paz-García, J.M. Feasibility Study of the Use of Different Extractant Agents in the Remediation of a Mercury Contaminated Soil from Almaden. *Sep. Purif. Technol.* **2011**, *79*, 151–156. [[CrossRef](#)]
46. Orecchio, S.; Polizzotto, G. Fractionation of mercury in sediments during draining of Augusta (Italy) coastal area by modified Tessier method. *Microchem. J.* **2013**, *110*, 452–457. [[CrossRef](#)]
47. Wasay, S.A.; Arnfalk, P.; Tokunaga, S. Remediation of a Soil Polluted by Mercury with Acidic Potassium Iodide. *J. Hazard. Mater.* **1995**, *44*, 93–102. [[CrossRef](#)]
48. Klasson, K.T.; Koran, L.J., Jr.; Gates, D.D.; Cameron, P.A. *Removal of Mercury from Solids Using the Potassium Iodide/Iodine Leaching Process*; Oak Ridge National Lab. (ORNL): Oak Ridge, TN, USA, 1997.
49. Ray, A.B.; Selvakumar, A. Laboratory studies on the remediation of mercury-contaminated soils. *Remediat. J.* **2000**, *10*, 49–56. [[CrossRef](#)]

50. Mauceri, A.; Fossi, M.C.; Leonzio, C.; Ancora, S.; Minniti, F.; Maisano, M.; Lo Cascio, P.; Ferrando, S.; Fasulo, S. Stress factors in the gills of *Liza aurata* (Perciformes, Mugilidae) living in polluted environments. *Ital. J. Zool.* **2005**, *72*, 285–292. [[CrossRef](#)]
51. Ellman, G.L.; Courtney, K.D.; Andres, V.; Featherstone, R.M. A new and rapid colorimetric determination of acetylcholinesterase activity. *Biochem. Pharmacol.* **1961**, *7*, 88–95. [[CrossRef](#)]
52. Benedetti, M.; Romano, E.; Ausili, A.; Fattorini, D.; Gorbi, S.; Maggi, C.; Salmeri, A.; Salvagio Manta, D.; Sesta, G.; Sprovieri, M.; et al. 10-year time course of Hg and organic compounds in Augusta Bay: Bioavailability and biological effects in marine organisms. *Front. Public Health* **2022**, *10*, 968296. [[CrossRef](#)] [[PubMed](#)]
53. Gilmour, C.C.; Henry, E.A.; Mitchell, R. Sulfate stimulation of mercury methylation in freshwater sediments. *Environ. Sci. Technol.* **1992**, *26*, 2281–2287. [[CrossRef](#)]
54. van den Berg, G.A.; Buykx, S.E.J.; van den Hoop, M.A.G.T.; van der Heijdt, L.M.; Zwolsman, J.J.G. Vertical profiles of trace metals and acid-volatile sulphide in a dynamic sedimentary environment: Lake Ketel, The Netherlands. *Appl. Geochem.* **2001**, *16*, 781–791. [[CrossRef](#)]
55. García-Ordiales, E.; Covelli, S.; Braidotti, G.; Petranich, E.; Pavoni, E.; Acquavita, A.; Sanz-Prada, L.; Roqueñí, N.; Loredó, J. Mercury and arsenic mobility in resuspended contaminated estuarine sediments (Asturias, Spain): A laboratory-based study. *Sci. Tot. Env.* **2020**, *744*, 140870. [[CrossRef](#)]
56. Bonsignore, M.; Tamburrino, S.; Oliveri, E.; Marchetti, A.; Durante, C.; Berni, A.; Quinci, E.; Sprovieri, M. Tracing Mercury Pathways in Augusta Bay (Southern Italy) by Total Concentration and Isotope Determination. *Environ. Pollut.* **2015**, *205*, 178–185. [[CrossRef](#)]
57. Cappello, T.; Maisano, M.; Giannetto, A.; Parrino, V.; Mauceri, A.; Fasulo, S. Neurotoxicological Effects on Marine Mussel *Mytilus Galloprovincialis* Caged at Petrochemical Contaminated Areas (Eastern Sicily, Italy): ¹H NMR and Immunohistochemical Assays. *Comp. Biochem. Physiol. Part C Toxicol. Pharmacol.* **2015**, *169*, 7–15. [[CrossRef](#)] [[PubMed](#)]
58. Maisano, M.; Cappello, T.; Natalotto, A.; Vitale, V.; Parrino, V.; Giannetto, A.; Oliva, S.; Mancini, G.; Cappello, S.; Mauceri, A.; et al. Effects of Petrochemical Contamination on Caged Marine Mussels Using a Multi-Biomarker Approach: Histological Changes, Neurotoxicity and Hypoxic Stress. *Mar. Environ. Res.* **2017**, *128*, 114–123. [[CrossRef](#)]
59. Cappello, T.; Mauceri, A.; Corsaro, C.; Maisano, M.; Parrino, V.; Lo Paro, G.; Messina, G.; Fasulo, S. Impact of environmental pollution on caged mussels *Mytilus galloprovincialis* using NMR-based metabolomics. *Mar. Pollut. Bull.* **2013**, *77*, 132–139. [[CrossRef](#)]
60. Humphries, J.E.; Yoshino, T.P. Cellular receptors and signal transduction in molluscan hemocytes: Connections with the innate immune system of vertebrates. *Integr. Comp. Biol.* **2003**, *43*, 305–312. [[CrossRef](#)]
61. Franzellitti, S.; Fabbri, E. Cyclic-AMP mediated regulation of ABCB mRNA expression in mussel haemocytes. *PLoS ONE* **2013**, *8*, e61634. [[CrossRef](#)] [[PubMed](#)]
62. Gosselin, R.E. The cilioexcitatory activity of serotonin. *J. Cell. Comp. Physiol.* **1961**, *58*, 17–25. [[CrossRef](#)] [[PubMed](#)]
63. Carroll, M.A.; Catapane, E.J. The nervous system control of lateral ciliary activity of the gill of the bivalve mollusc, *Crassostrea virginica*. *Comp. Biochem. Physiol. A Mol. Integr. Physiol.* **2007**, *148*, 445–450. [[CrossRef](#)]
64. Matozzo, V.; Tomei, A.; Marin, M. Acetylcholinesterase as a biomarker of exposure to neurotoxic compounds in the clam *Tapes philippinarum* from the Lagoon of Venice. *Mar. Pollut. Bull.* **2005**, *50*, 1686–1693. [[CrossRef](#)]
65. Lionetto, M.G.; Caricato, R.; Calisi, A.; Giordano, M.E.; Schettino, T. Acetylcholinesterase as a biomarker in environmental and occupational medicine: New insights and future perspectives. *Biomed. Res. Int.* **2013**, *2013*, 321213. [[CrossRef](#)] [[PubMed](#)]

Disclaimer/Publisher’s Note: The statements, opinions and data contained in all publications are solely those of the individual author(s) and contributor(s) and not of MDPI and/or the editor(s). MDPI and/or the editor(s) disclaim responsibility for any injury to people or property resulting from any ideas, methods, instructions or products referred to in the content.